Gas Sensors Based on Titanium Oxides

Subjects: Materials Science, Coatings & Films

Contributor: Simonas Ramanavičius , Arūnas Ramanavičius , Arūnas Jagminas

Nanostructured titanium compounds have recently been applied in the design of gas sensors. Among titanium compounds, titanium oxides (TiO_2) are the most frequently used in gas sensing devices. Very recently, the applicability of non-stoichiometric titanium oxide (TiO_{2-x})-based layers for the design of gas sensors was demonstrated. The most promising titanium compounds and hetero- and nano-structures based on these compounds are discussed and the possibility to tune the sensitivity and selectivity of titanium compound-based sensing layers is addressed.

titanium dioxide (TiO) | non-stoichiometric titanium oxide (TiO or TiO) | magneli phases (TiO) | gas and volatile organic compounds (VOCs) sensors

1. Structural Features and Physicochemical Properties of Stoichiometric and Non-Stoichiometric Titanium Oxides

TiO_2 belongs to n-type semiconducting materials [1]. Many TiO_2-based heterostructures are used in the design of sensors [2][3] and biosensors [4][5]. However, all the most popular forms of titanium oxides are characterized by specific bandgaps, which are as follows: (i) anatase by 3.02 eV (ii) rutile by 3.23 eV; (iii) brookite by 2.96 eV [6]. The annealing procedure is mostly used for the conversion of one titanium oxide phase into another one. Besides stoichiometric titanium oxide, plenty of non-stoichiometric forms were identified, among them very attractive conducting/semiconducting characteristics and gas-sensing properties [3]. They have Magnéli phases, which are described by Ti_nO_{2n-1} stoichiometry, where n = 4, …, 10. Their Magnéli phase neighbor is titanium pentoxide (Ti_3O_5), where n = 3 with a stoichiometry of Ti_nO_{2n-1}, which appears in a variety of different forms (that are indicated as α−, β−, γ−, δ−, and λ−) [7]. Stoichiometry of titanium pentoxide corresponds to that of the Magnéli phases (Ti_nO_{2n-1}). Titanium pentoxide forms monoclinic crystals with the following lattice constants: a = 9.9701 Å, b = 5.0747 Å, c = 7.1810 Å, β = 109.865°. Moreover, titanium pentoxide, as well as some other Magnéli phases (e.g., Ti_4O_7), exhibit superconductivity when cooled down below 7 K temperature [8].

The most significant difference between titanium pentoxide and the Magnéli phases is determined by their different crystal structures. Magnéli phases contains shear planes based on $TiO_{2(rutile)}$ [9], while in titanium pentoxide, such planes are absent [3][8]. A temperature of 400 °C is optimal for the appearance of $TiO_{2(anatase)}$ intergrowths within Ti_3O_5 crystals based on TiO_{2-x}/TiO_2-based heterostructures [10]. The incorporation of intergrowths based on $TiO_{2(anatase)}$ in the structure of titanium pentoxide (Ti_3O_5) improves their conductivity and some photoluminescence-

related characteristics [3]. It should be noted that such non-stoichiometric titanium oxides can be spontaneously oxidized for this reason and significant attention should be paid to the stabilization of these structures during their usage in the development of gas sensors. It should be noted that at different oxidation states, titanium oxides have different crystal structures [11][12], which starts from rutile for TiO_2 and anatase for $Ti_{10}O_{19}$ and then it turns into the triclinic structure for many stoichiometries, ranging from Ti_9O_{17} until Ti_4O_7, monoclinic for γTi_3O_5, tetragonal for Ti_2O_3 and hexagonal for TiO, Ti_2O and metallic titanium.

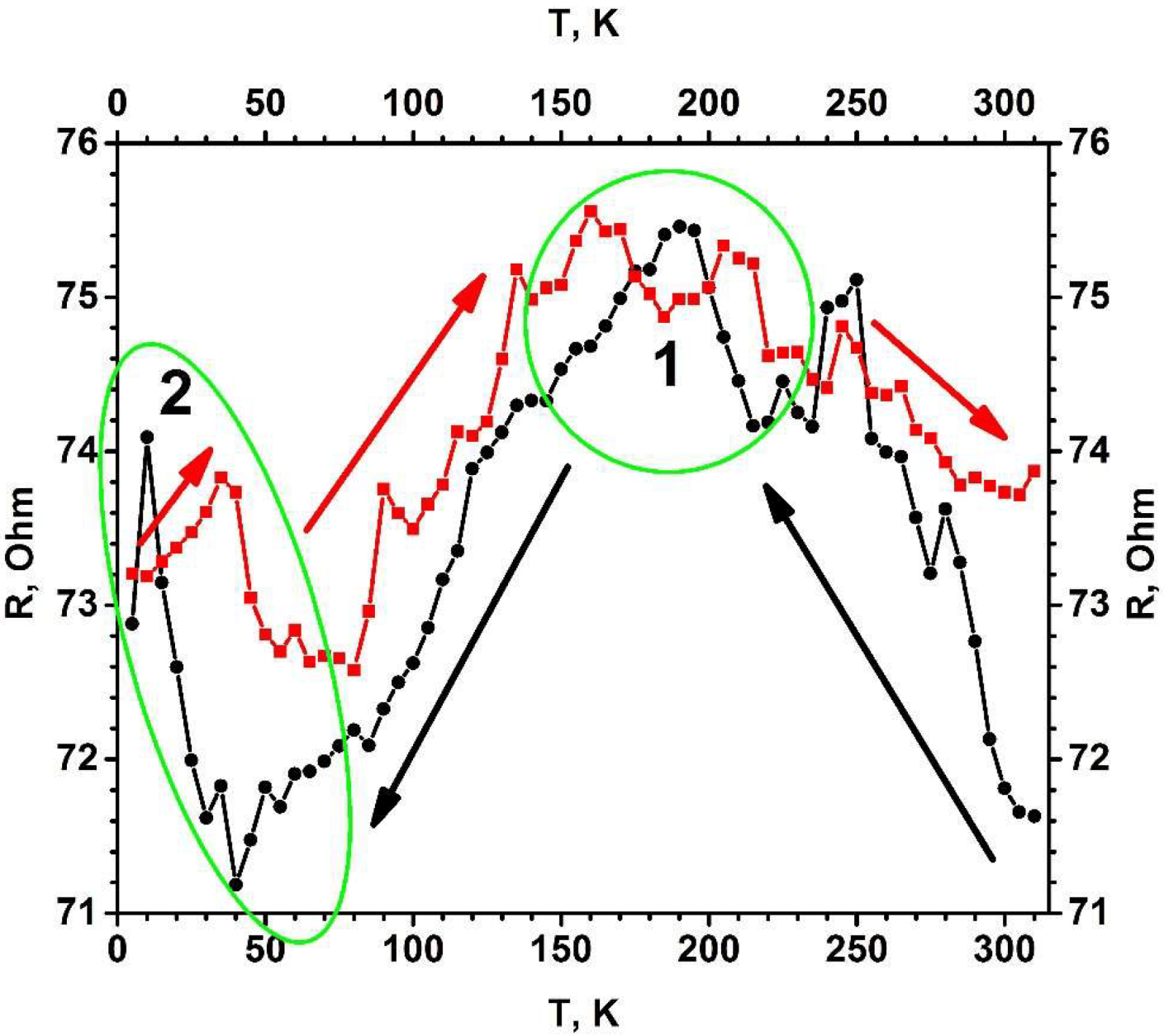

Figure 1. Temperature dependence of electrical resistance (R(T)) for the TiO_{2-x}/TiO_2(400 °C)-based hetero-structure. Temperature was changed in two ways (indicated by black and red arrows): (i) black cycles shows points measured by cooling down, (ii) red squares shows points by increasing temperature. Measurements were performed in vacuum using helium cryostat. Figure adapted from [3].

The electrical conductivity of most non-stoichiometric titanium oxides is significantly higher than the conductivity of any allotropic form of stoichiometric titanium oxides (TiO_2). The most significant increase in sensitivity is observed for titanium oxides with Ti_nO_{2n-1} stoichiometry, when index 'n' is in the range of 4–10 [13]. Some compounds with the above-mentioned stoichiometry form Magnéli phases, which are characterized by metallic conductivity and even by superconductivity [14].

Non-stoichiometric titanium oxide-based layers based on Magnéli phases have well conducting intergrowths based on Ti_nO_{2n-1} planar moieties that penetrate the TiO_2-based matrix [3]. Non-stoichiometric titanium oxides, such as Ti_2O_3 and/or Ti_3O_5, which do not form real Magnéli phases anyway, are much better at conducting in comparison to stoichiometric TiO_2 [3][8]. These n-type semiconducting titanium oxides have a high concentration of 'oxygen vacancies', which are responsible for the mobility of electrons through their structure [15] and baseline resistance [16]. It should be outlined that these 'oxygen vacancies' are also responsible for the sensitivity towards both oxidizing and reducing gases [3]. During the design of the sensing layer, initially formed stoichiometric titanium oxide-based layers can be chemically reduced into non-stoichiometric titanium oxide (TiO_{2-x}) and/or Magnéli phases [17]. Magnéli phases are observed when the oxygen concentration in TiO_{2-x} structure is decreased and 'x' value is between 0.1 and 0.34 [3][18]. Non-stoichiometric titanium oxide structures containing Magnéli phases are chemically stable and rather well conducting. For these reasons, they are often applied in wastewater treatment and the design of batteries and fuel cells [19][20]; the same characteristics are required for gas sensors.

Non-stoichiometric titanium oxide-based structures can be developed using several approaches, namely plasma-treatment [21], laser irradiation-based modification [22], reduction by metallic zinc [23], bombardment by high-energy particles [24] and thermo-chemical approaches [12]. However, the formation of large Ti_3O_5 monocrystals is rather challenging because titanium oxides are polymorphic [8]. In some situations, stoichiometric titanium oxide can be easily turned into a non-stoichiometric one by suitable doping and/or reduction.

During the formation of TiO_{2-x}/TiO_2-based heterostructures, the ratio between stoichiometric titanium oxide and non-stoichiometric titanium oxide can be significantly increased by thermal treatment in reducing the gas atmosphere [25]. In several works, the transition between the insulator state and metallic state of Ti_3O_5 (β and λ forms of Ti_3O_5, respectively) was performed by pulses of visible light [7] and by thermal treatment, which induced the conversion of α form into β form at 450 K [26] and the conversion of δ form into γ form at 240 K [7]. The phase transition of Ti_3O_5 at 240–450 K is the most important for the adjustment of conductivity of this semiconducting material-based layers, e.g., the switching between metal and insulator states was observed at 350 K [8].

In some situations, non-stoichiometric titanium oxide can be formed by the partial oxidation of metallic titanium layers, which is followed by thermal treatment and annealing [3]. Sensors based on such structures, which are differently thermally treated and annealed, can be used in the formation of sensors with very different selectivity and sensitivity, which are suitable for the development of sensor arrays. Non-stoichiometric titanium oxide-based sensors. despite some significant advantages related to better catalytic activity and conductivity, have some disadvantages in comparison to those based on stoichiometric titanium oxides related to their insufficient stability at ambient conditions. In addition, it should be noted that the selectivity of these sensors is not superior.

2. Pristine Titanium Oxide-Based Gas Sensors and Their Sensing Mechanisms

Stoichiometric TiO_2-based gas sensors show high sensitivity to different gases. It should be noted that TiO_2-based gas sensors can rely on several different sensing mechanisms, which differ the most significantly for the determination of reducing gaseous compounds, such as H_2, H_2S, NH_3, CO, CH_3OH, C_2H_5OH, etc. and for oxidizing gaseous compounds, such as O_2, NO_2, CO_2 [27][28][29]. The changes in electrical resistivity of the TiO_2-based layer are mostly used for the determination of analytical signals; therefore, the assessment of analytical signals generated by such sensors is rather simple. In some situations, measurement protocols were advanced by the determination of photoluminescence signals [3][17][30], which are generated by semiconducting TiO_2 structures [31]. Some above-mentioned photocatalytic and photovoltaic properties can be improved by laser-based treatment [32]. However, the main disadvantage of TiO_2-based sensors is poor selectivity towards gaseous materials, which significantly complicates the application of these analytical devices. Therefore, in order to improve selectivity, various heterostructures containing TiO_2 hybridized with many other semiconductors have been developed [33], e.g., the research group has developed a TiO_{2-x}/TiO_2-based self-heating heterostructure for the determination of NH_3, CH_3OH and C_2H_5OH [3].

Table 1. Characteristics of titanium oxide-based sensors [34].

Sensing Material	Working Temperature	Gas Concentration	Response Value (R_a/R_g) or (($\Delta R/R_g$) × 100%)	Response Time	Recovery Time	Reference
TiO_2 (rutile), Ti_8O_{15} and Ti_9O_{17} mixture	210 °C	12.5–100 ppm (NH_3)	1–7%	2 min	8 min	[35]
TiO_x-NiO	250–350 °C	100 ppm (H_2) 100 ppm (NO_2) 100 ppm (NH_3)	17 for H_2 (250 °C) 16 for NO_2 (250 °C)	2 min	2,3 min	[36]

			4 for NH_3 (250 °C)			
β-Ti_3O_5	150 °C	50 ppm (H_2)	11%	-	-	[37]
Ti_3O_5-TiO_2 mixture	25–180 °C	105 ppm (H_2O) 118 ppm (methanol) 53 ppm (ethanol) 18 ppm n-propanol 220 ppm (acetone)	0.5–18%	-	4–35 s	[3]
TiO_2-Ti_6O	150–450 °C	2000 pm (H_2) 20 ppm (NO_2) 500 ppb (O_3) 1.6 ppm (acetone) 80 ppm (NO_x)	2.9–348	8–21 s	20–32 s	[2]
Ti^{3+}-TiO_2	RT	100 ppm (CO)	39%	10 s	30 s	[38]
TiO_2	150 °C	100 ppm (ethanol)	75.4%	155 s	779 s	[39]
TiO_2	270 °C	500 ppm (acetone)	9.19	10 s	9 s	[40]

TiO_2	350 °C	400 ppm (ethanol)	22.9	5 s	7 s	[41]
TiO_2	RT	200 ppm (NH_3)	64	28 s	24 s	[42]
α-Fe_2O_3-TiO_2	325 °C	100 ppm (ethanol)	4	46 s	16 s	[43]

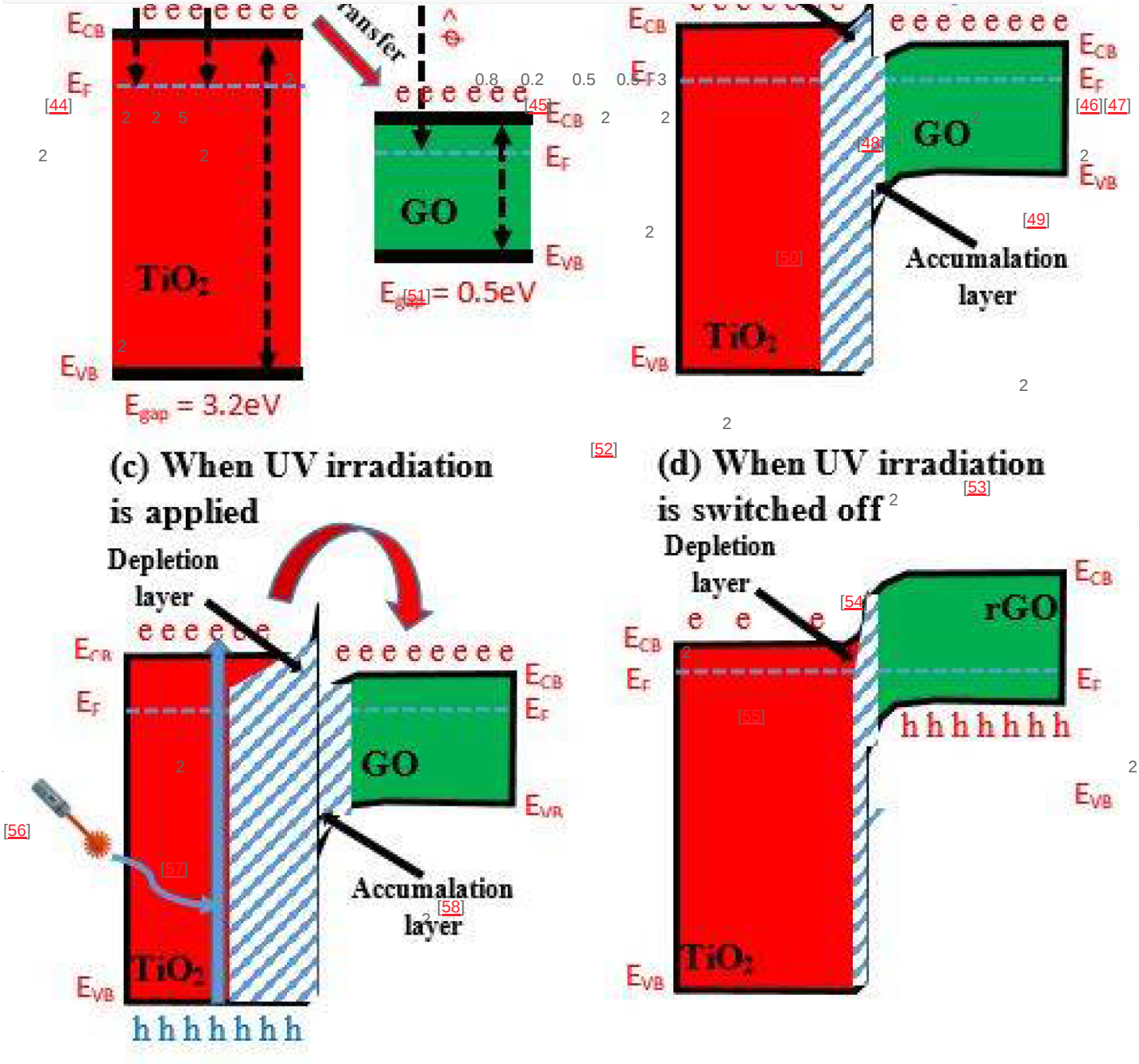

Figure 2. Band diagram of TiO_2/GO hetero-structure (**a**) before the formation of hetero-structure, (**b**) after the formation of hetero-structure, (**c**) when UV irradiation is applied, and (**d**) when UV irradiation is switched off. ('e' is an electron; 'h' is a hole) [34].

The heterostructure based on TiO_2/SnO_2 is also very interesting because the depletion of energetic layers in the molecular orbitals of TiO_2 electrons is induced when TiO_2 is connected to SnO_2 [46]. It should be noted that nanoparticle-based structures are preferable for the development of gas sensors [59] because the radius of nanoparticles based on some semiconducting materials that are used in the design of gas-sensors are in the same range as the Exciton Bohr radius; for this reason, such particles are very suitable for the design of gas sensors [60].

SnO_2 has great charge-carrier mobility, which is the most important factor for gas sensors based on resistivity measurements [47]. SnO_2-based gas-sensing layers are cheap and stable at ambient conditions [61] however, it should be taken into account that sensors based on stoichiometric TiO_2 and SnO_2 operate at a rather high temperature, which exceeds several hundred degrees [60]. However, such sensors consume a lot of energy for the heating of the sensing layer; therefore, due to energy saving related issues, sensing layers capable to operate at low temperatures are under very special interest, e.g., sensing layers based on Au/SnO_2 core-shell structures can operate in the temperature interval of 25–80 °C [62]. The investigations of non-stoichiometric titanium oxide-based sensors shows that these sensors can operate even at room temperature [3][17]. It is expected that heterostructures based on SnO_2/TiO_2 can be applied in low temperature gas sensors; therefore, some nanostructures were designed, which are as follows: TiO_2 nanobelts covered by SnO_2 [63], TiO_2/SnO_2-based core-shell nanofibers [64], SnO_2 layers doped by TiO_2 [65], structures based on SnO_2/TiO_2 laminates [66], SnO_2 nanoparticles wrapped within TiO_2-based nanofibers [46], SnO_2-based quantum dots formed on a surface of TiO_2 layer were reported to be sensitive towards NO_2 and CO [67]. Atomic layer deposition (ALD) was used to deposit thin TiO_2 layers and it was demonstrated that tuning of the selectivity can be performed by the adjustment of TiO_2 layer thickness [68].

Significant energy consumptions for the heating of the sensing layer reduce the applicability of most gas sensors. Therefore, there is a demand for gas-sensing structures that can operate at low temperatures [69]. The miniaturization of sensing elements is another suitable strategy to reduce energy consumption. Low-temperature sensors based on titanium oxide-based layers were reported for O_2 [66], ozone [45], formaldehyde [70], CO [44], ethanol [65], C_7H_8 [48], H_2 [71] and other gases [72].

The 'self-heating' of the sensing layer can be achieved when it has rather low resistance and part of electrical energy, which passes through this layer and is converted into thermal energy [3][17]. However, stoichiometric titanium oxide-based layers are characterised by a high band gap; therefore, the conductivity of these layers is not sufficient for 'self-heating' because rather high voltages are required to achieve some effect. On the contrary, this operation mode is very suitable for non-stoichiometric titanium oxide-based sensors, because these layers are good at conducting at low temperatures and in the temperature interval of 72–180 °C, these layers reach very good sensitivity towards some gases [3][17]. The semiconducting properties and chemical activity of titanium oxide enable sufficient catalytic and photocatalytic activities under UV irradiation to turn into a 'water splitting' ability [32], which eventually can be exploited for sensing purposes. It should be noted that at room temperature (298 K), sensing

layers are sensitive to humidity. Therefore, analytical signals generated by adsorbed water molecules interfere with an analytical signal generated by target gases.

References

1. Yamazoe, N.; Sakai, G.; Shimanoe, K. Oxide Semiconductor Gas Sensors. Catal. Surv. Asia 2003, 7, 63–75.
2. Maziarz, W.; Kusior, A.; Trenczek-Zajac, A. Nanostructured TiO2-Based Gas Sensors with Enhanced Sensitivity to Reducing Gases. Beilstein J. Nanotechnol. 2016, 7, 1718–1726.
3. Ramanavicius, S.; Tereshchenko, A.; Karpicz, R.; Ratautaite, V.; Bubniene, U.; Maneikis, A.; Jagminas, A.; Ramanavicius, A. TiO2-x/TiO2-Structure Based ‘Self-Heated’ Sensor for the Determination of Some Reducing Gases. Sensors 2020, 20, 74.
4. Tereshchenko, A.; Smyntyna, V.; Ramanavicius, A. Interaction Mechanism between TiO2 Nanostructures and Bovine Leukemia Virus Proteins in Photoluminescence-Based Immunosensors. RSC Adv. 2018, 8, 37740–37748.
5. Tereshchenko, A.; Viter, R.; Konup, I.; Ivanitsa, V.; Geveliuk, S.; Ishkov, Y.; Smyntyna, V. TiO2 Optical Sensor for Amino Acid Detection. In Proceedings of the Biophotonics—Riga 2013, Riga, Latvia, 26–31 August 2013; Spigulis, J., Kuzmina, I., Eds.; SPIE: Washington, DC, USA, 2013; Volume 9032, pp. 186–190.
6. Wunderlich, W.; Oekermann, T.; Miao, L.; Hue, N.T.; Tanemura, S.; Tanemura, M. ELECTRONIC PROPERTIES OF NANO-POROUS TiO 2- AND ZnO THIN FILMS- COMPARISON OF SIMULATIONS AND EXPERIMENTS. J. Ceram. Process. Res. 2004, 5, 343–354.
7. Ohkoshi, S.; Tsunobuchi, Y.; Matsuda, T.; Hashimoto, K.; Namai, A.; Hakoe, F.; Tokoro, H. Synthesis of a Metal Oxide with a Room-Temperature Photoreversible Phase Transition. Nat. Chem. 2010, 2, 539–545.
8. Yoshimatsu, K.; Sakata, O.; Ohtomo, A. Superconductivity in Ti4O7 and γ-Ti3O5 Films. Sci. Rep. 2017, 7, 12544.
9. Marezio, M.; McWhan, D.B.; Dernier, P.D.; Remeika, J.P. Structural Aspects of the Metal-Insulator Transitions in Ti4O7. J. Solid State Chem. 1973, 6, 213–221.
10. D’Angelo, A.M.; Webster, N.A.S. Evidence of Anatase Intergrowths Formed during Slow Cooling of Reduced Ilmenite. J. Appl. Crystallogr. 2018, 51, 185–192.
11. Jayashree, S.; Ashokkumar, M. Switchable Intrinsic Defect Chemistry of Titania for Catalytic Applications. Catalysts 2018, 8, 601.

12. Arūnas Jagminas; Simonas Ramanavičius; Vitalija Jasulaitiene; Mantas Šimėnas; Hydrothermal synthesis and characterization of nanostructured titanium monoxide films. *RSC Advances* **2019**, *9*, 40727-40735, 10.1039/c9ra08463k.
13. Andersson, S.; Magnéli, A. Diskrete Titanoxydphasen Im Zusammensetzungsbereich TiO_1,75-TiO_1,90. Naturwissenschaften 1956, 43, 495–496.
14. Liborio, L.; Mallia, G.; Harrison, N. Electronic Structure of the Ti4O7 Magneli Phase. Phys. Rev. B 2009, 79, 245133.
15. Zhu, Q.; Peng, Y.; Lin, L.; Fan, C.-M.; Gao, G.-Q.; Wang, R.-X.; Xu, A.-W. Stable Blue TiO2−x Nanoparticles for Efficient Visible Light Photocatalysts. J. Mater. Chem. A 2014, 2, 4429–4437.
16. Al-Hashem, M.; Akbar, S.; Morris, P. Role of Oxygen Vacancies in Nanostructured Metal-Oxide Gas Sensors: A Review. Sens. Actuators B Chem. 2019, 301, 126845.
17. Ramanavicius, S.; Ramanavicius, A. Insights in the Application of Stoichiometric and Non-Stoichiometric Titanium Oxides for the Design of Sensors for the Determination of Gases and VOCs (TiO2−x and TinO2n−1 vs. TiO2). Sensors 2020, 20, 6833.
18. Harada, S.; Tanaka, K.; Inui, H. Thermoelectric Properties and Crystallographic Shear Structures in Titanium Oxides of the Magnèli Phases Bandgap Engineering of Magnéli Phase TinO2n−1: Electron-Hole Self-Compensation. J. Appl. Phys. 2010, 108, 83703.
19. Walsh, F.C.; Wills, R.G.A. The Continuing Development of Magnéli Phase Titanium Sub-Oxides and Ebonex® Electrodes. Electrochim. Acta 2010, 55, 6342–6351.
20. Arūnas Jagminas; Arnas Naujokaitis; Paulius Gaigalas; Simonas Ramanavičius; Marija Kurtinaitienė; Romualdas Trusovas; Substrate Impact on the Structure and Electrocatalyst Properties of Molybdenum Disulfide for HER from Water. *Metals* **2020**, *10*, 1251, 10.3390/met10091251.
21. Nakamura, I.; Negishi, N.; Kutsuna, S.; Ihara, T.; Sugihara, S.; Takeuchi, K. Role of Oxygen Vacancy in the Plasma-Treated TiO2 Photocatalyst with Visible Light Activity for NO Removal. J. Mol. Catal. A Chem. 2000, 161, 205–212.
22. le Mercier, T.; Mariot, J.M.; Parent, P.; Fontaine, M.F.; Hague, C.F.; Quarton, M. Formation of Ti3+ Ions at the Surface of Laser-Irradiated Rutile. Appl. Surf. Sci. 1995, 86, 382–386.
23. Zheng, Z.; Huang, B.; Meng, X.; Wang, J.; Wang, S.; Lou, Z.; Wang, Z.; Qin, X.; Zhang, X.; Dai, Y. Metallic Zinc- Assisted Synthesis of Ti3+ Self-Doped TiO2 with Tunable Phase Composition and Visible-Light Photocatalytic Activity. Chem. Commun. 2013, 49, 868–870.
24. Hashimoto, S.; Tanaka, A. Alteration of Ti 2p XPS Spectrum for Titanium Oxide by Low-Energy Ar Ion Bombardment. Surf. Interface Anal. 2002, 34, 262–265.

25. Hayfield, P.C.S. Development of a New Material: Monolithic Ti4O7 Ebonex Ceramic; Royal Society of Chemistry: London, UK, 2007; ISBN 184755069X.
26. Åsbrink, S.; Magnéli, A. Crystal Structure Studies on Trititanium Pentoxide, Ti3O5. Acta Crystallogr. 1959, 12, 575–581.
27. Linsebigler, A.L.; Lu, G.; Yates, J.T. Photocatalysis on TiO2 Surfaces: Principles, Mechanisms, and Selected Results. Chem. Rev. 1995, 95, 735–758.
28. Wang, Y.; Du, G.; Liu, H.; Liu, D.; Qin, S.; Wang, N.; Hu, C.; Tao, X.; Jiao, J.; Wang, J.; et al. Nanostructured Sheets of Ti—O Nanobelts for Gas Sensing and Antibacterial Applications. Adv. Funct. Mater. 2008, 18, 1131–1137.
29. Kimura, M.; Sakai, R.; Sato, S.; Fukawa, T.; Ikehara, T.; Maeda, R.; Mihara, T. Sensing of Vaporous Organic Compounds by TiO2 Porous Films Covered with Polythiophene Layers. Adv. Funct. Mater. 2012, 22, 469–476.
30. Petruleviciene, M.; Juodkazyte, J.; Parvin, M.; Tereshchenko, A.; Ramanavicius, S.; Karpicz, R.; Samukaite-Bubniene, U.; Ramanavicius, A. Tuning the Photo-Luminescence Properties of WO3 Layers by the Adjustment of Layer Formation Conditions. Materials 2020, 13, 2814.
31. Viter, R.; Tereshchenko, A.; Smyntyna, V.; Ogorodniichuk, J.; Starodub, N.; Yakimova, R.; Khranovskyy, V.; Ramanavicius, A. Toward Development of Optical Biosensors Based on Photoluminescence of TiO2 Nanoparticles for the Detection of Salmonella. Sens. Actuators B Chem. 2017, 252, 95–102.
32. Haryński, Ł.; Grochowska, K.; Karczewski, J.; Ryl, J.; Siuzdak, K. Scalable Route toward Superior Photoresponse of UV-Laser-Treated TiO2 Nanotubes. ACS Appl. Mater. Interfaces 2020, 12, 3225–3235.
33. Simonas Ramanavicius, Arunas Ramanavicius; Development of molecularly imprinted polymer based phase boundaries for sensors design (review). *Advances in Colloid and Interface Science* **2022**, *305*, 102693, 10.1016/j.cis.2022.102693.
34. Simonas Ramanavicius; Arunas Jagminas; Arunas Ramanavicius; Gas Sensors Based on Titanium Oxides (Review). *Coatings* **2022**, *12*, 699, 10.3390/coatings12050699.
35. M. Gardon; O. Monereo; S. Dosta; G. Vescio; A. Cirera; J.M. Guilemany; New procedures for building-up the active layer of gas sensors on flexible polymers. *Surface and Coatings Technology* **2013**, *235*, 848-852, 10.1016/j.surfcoat.2013.09.011.
36. C Imawan; F Solzbacher; H Steffes; E Obermeier; TiOx-modified NiO thin films for H2 gas sensors: effects of TiOx-overlayer sputtering parameters. *Sensors and Actuators B: Chemical* **2000**, *68*, 184-188, 10.1016/s0925-4005(00)00427-5.

37. Xiaolei Li; Ying Liu; Shiqing Ma; Jinwen Ye; Xiaoyan Zhang; Guangrui Wang; Yuchong Qiu; The synthesis and gas sensitivity of the beta-Ti3O5 powder: Experimental and DFT study. *Journal of Alloys and Compounds* **2015**, *649*, 939-948, 10.1016/j.jallcom.2015.07.094.
38. Juan Su; Xiao-Xin Zou; Yong-Cun Zou; Guo-Dong Li; Pei-Pei Wang; Jie-Sheng Chen; Porous Titania with Heavily Self-Doped Ti3+ for Specific Sensing of CO at Room Temperature. *Inorganic Chemistry* **2013**, *52*, 5924-5930, 10.1021/ic400109j.
39. Teena Gakhar; Arnab Hazra; Oxygen vacancy modulation of titania nanotubes by cathodic polarization and chemical reduction routes for efficient detection of volatile organic compounds. *Nanoscale* **2020**, *12*, 9082-9093, 10.1039/c9nr10795a.
40. Sachin Navale; Z.B. Yang; Chenshitao Liu; P.J. Cao; V.B. Patil; N.S. Ramgir; Rajaram Mane; F.J. Stadler; Enhanced acetone sensing properties of titanium dioxide nanoparticles with a sub-ppm detection limit. *Sensors and Actuators B: Chemical* **2017**, *255*, 1701-1710, 10.1016/j.snb.2017.08.186.
41. Xue Gao; Yanqiong Li; Wen Zeng; Caifeng Zhang; Yaoming Wei; Hydrothermal synthesis of agglomerating TiO2 nanoflowers and its gas sensing. *Journal of Materials Science: Materials in Electronics* **2017**, *28*, 18781-18786, 10.1007/s10854-017-7827-0.
42. Neli Mintchevaac; Parthasarathy Srinivasanb; John Bosco Balaguru Rayappan; Aleksandr A.Kuchmizhakde; Stanislav Gurbatovde; Sergei Kulinich; Room-temperature gas sensing of laser-modified anatase TiO2 decorated with Au nanoparticles. *Applied Surface Science* **2019**, *507*, 145169, 10.1016/j.apsusc.2019.145169.
43. Hui Mei; Shixiang Zhou; Mingyang Lu; Yong Zhao; Laifei Cheng; Construction of pine-branch-like alpha-Fe2O3/TiO2 hierarchical heterostructure for gas sensing. *Ceramics International* **2020**, *46*, 18675-18682, 10.1016/j.ceramint.2020.04.181.
44. Hsu, K.C.; Fang, T.H.; Hsiao, Y.J.; Wu, P.C. Response and Characteristics of TiO2/Perovskite Heterojunctions for CO Gas Sensors. J. Alloys Compd. 2019, 794, 576–584.
45. Avansi, W.; Catto, A.C.; da Silva, L.F.; Fiorido, T.; Bernardini, S.; Mastelaro, V.R.; Aguir, K.; Arenal, R. One-Dimensional V2O5/TiO2 Heterostructures for Chemiresistive Ozone Sensors. ACS Appl. Nano Mater. 2019, 2, 4756–4764.
46. Chen, K.; Chen, S.; Pi, M.; Zhang, D. SnO2 Nanoparticles/TiO2 Nanofibers Heterostructures: In Situ Fabrication and Enhanced Gas Sensing Performance. Solid-State Electron. 2019, 157, 42–47.
47. Yu, Q.; Zhu, J.; Xu, Z.; Huang, X. Facile Synthesis of α-Fe2O3@SnO2 Core–Shell Heterostructure Nanotubes for High Performance Gas Sensors. Sens. Actuators B Chem. 2015, 213, 27–34.

48. Seekaew, Y.; Wisitsoraat, A.; Phokharatkul, D.; Wongchoosuk, C. Room Temperature Toluene Gas Sensor Based on TiO2 Nanoparticles Decorated 3D Graphene-Carbon Nanotube Nanostructures. Sens. Actuators B Chem. 2019, 279, 69–78.
49. Stratakis, E.; Savva, K.; Konios, D.; Petridis, C.; Kymakis, E. Improving the Efficiency of Organic Photovoltaics by Tuning the Work Function of Graphene Oxide Hole Transporting Layers. Nanoscale 2014, 6, 6925–6931.
50. Chen, C.; Cai, W.; Long, M.; Zhou, B.; Wu, Y.; Wu, D.; Feng, Y. Synthesis of Visible-Light Responsive Graphene Oxide/TiO2 Composites with p/n Heterojunction. ACS Nano 2010, 4, 6425–6432.
51. Lightcap, I.V.; Kosel, T.H.; Kamat, P. Anchoring Semiconductor and Metal Nanoparticles on a Two-Dimensional Catalyst Mat. Storing and Shuttling Electrons with Reduced Graphene Oxide. Nano Lett. 2010, 10, 577–583.
52. Lam, K.C.; Huang, B.; Shi, S.-Q. Room-Temperature Methane Gas Sensing Properties Based on in Situ Reduced Graphene Oxide Incorporated with Tin Dioxide. J. Mater. Chem. A 2017, 5, 11131–11142.
53. Ye, Z.; Tai, H.; Xie, T.; Yuan, Z.; Liu, C.; Jiang, Y. Room Temperature Formaldehyde Sensor with Enhanced Performance Based on Reduced Graphene Oxide/Titanium Dioxide. Sens. Actuators B Chem. 2016, 223, 149–156.
54. Buchsteiner, A.; Lerf, A.; Pieper, J. Water Dynamics in Graphite Oxide Investigated with Neutron Scattering. J. Phys. Chem. B 2006, 110, 22328–22338.
55. Phan, D.T.; Chung, G.S. Effects of Rapid Thermal Annealing on Humidity Sensor Based on Graphene Oxide Thin Films. Sens. Actuators B Chem. 2015, 220, 1050–1055.
56. Wang, P.; Zhai, Y.; Wang, D.; Dong, S. Synthesis of Reduced Graphene Oxide-Anatase TiO2 Nanocomposite and Its Improved Photo-Induced Charge Transfer Properties. Nanoscale 2011, 3, 1640–1645.
57. Cui, S.; Wen, Z.; Huang, X.; Chang, J.; Chen, J. Stabilizing MoS2 Nanosheets through SnO2 Nanocrystal Decoration for High-Performance Gas Sensing in Air. Small 2015, 11, 2305–2313.
58. Lee, E.; Lee, D.; Yoon, J.; Yin, Y.; Lee, Y.N.; Uprety, S.; Yoon, Y.S.; Kim, D.-J. Enhanced Gas-Sensing Performance of GO/TiO2 Composite by Photocatalysis. Sensors 2018, 18, 3334.
59. Mirzaei, A.; Janghorban, K.; Hashemi, B.; Bonavita, A.; Bonyani, M.; Leonardi, S.G.; Neri, G. Synthesis, Characterization and Gas Sensing Properties of α-Fe2O3 Core–Shell Nanocomposites. Nanomaterials 2015, 5, 737–749.
60. Mosadegh Sedghi, S.; Mortazavi, Y.; Khodadadi, A. Low Temperature CO and CH4 Dual Selective Gas Sensor Using SnO2 Quantum Dots Prepared by Sonochemical Method. Sens. Actuators B

Chem. 2010, 145, 7–12.

61. Rieu, M.; Camara, M.; Tournier, G.; Viricelle, J.P.; Pijolat, C.; de Rooij, N.F.; Briand, D. Fully Inkjet Printed SnO2 Gas Sensor on Plastic Substrate. Sens. Actuators B Chem. 2016, 236, 1091–1097.
62. Chung, F.C.; Wu, R.J.; Cheng, F.C. Fabrication of a 2 Core–Shell Structure for Gaseous Formaldehyde Sensing at Room Temperature. Sens. Actuators B Chem. 2014, 190, 1–7.
63. Chen, G.; Ji, S.; Li, H.; Kang, X.; Chang, S.; Wang, Y.; Yu, G.; Lu, J.; Claverie, J.; Sang, Y.; et al. High-Energy Faceted SnO2-Coated TiO2 Nanobelt Heterostructure for Near-Ambient Temperature-Responsive Ethanol Sensor. ACS Appl. Mater. Interfaces 2015, 7, 24950–24956.
64. Li, F.; Gao, X.; Wang, R.; Zhang, T.; Lu, G. Study on TiO2-SnO2 Core-Shell Heterostructure Nanofibers with Different Work Function and Its Application in Gas Sensor. Sens. Actuators B Chem. 2017, 248, 812–819.
65. Zeng, W.; Liu, T.; Wang, Z. UV Light Activation of TiO2 Doped SnO2 Thick Film for Sensing Ethanol at Room Temperature. Mater. Trans. 2010, 51, 243–245.
66. Lee, H.C.; Hwang, W.S. Substrate Effects on the Oxygen Gas Sensing Properties of SnO2/TiO2 Thin Films. Appl. Surf. Sci. 2006, 253, 1889–1897.
67. Lee, J.H.; Mirzaei, A.; Kim, J.H.; Kim, J.Y.; Nasriddinov, A.F.; Rumyantseva, M.N.; Kim, H.W.; Kim, S.S. Gas-Sensing Behaviors of TiO2-Layer-Modified SnO2 Quantum Dots in Self-Heating Mode and Effects of the TiO2 Layer. Sens. Actuators B Chem. 2020, 310, 127870.
68. Ng, S.; Prášek, J.; Zazpe, R.; Pytlíček, Z.; Spotz, Z.; Pereira, J.R.; Michalička, J.; Přikryl, J.; Krbal, M.; Sopha, H.; et al. Atomic Layer Deposition of SnO2-Coated Anodic One-Dimensional TiO2 Nanotube Layers for Low Concentration NO2 Sensing. ACS Appl. Mater. Interfaces 2020, 12, 33386–33396.
69. Song, Z.; Wei, Z.; Wang, B.; Luo, Z.; Xu, S.; Zhang, W.; Yu, H.; Li, M.; Huang, Z.; Zang, J.; et al. Sensitive Room-Temperature H2S Gas Sensors Employing SnO2 Quantum Wire/Reduced Graphene Oxide Nanocomposites. Chem. Mater. 2016, 28, 1205–1212.
70. Nasriddinov, A.; Rumyantseva, M.; Marikutsa, A.; Gaskov, A.; Lee, J.-H.; Kim, J.-H.; Kim, J.-Y.; Kim, S.S.; Kim, H.W. Sub-Ppm Formaldehyde Detection by n-n TiO2@SnO2 Nanocomposites. Sensors 2019, 19, 3182.
71. Shaposhnik, D.; Pavelko, R.; Llobet, E.; Gispert-Guirado, F.; Vilanova, X. Hydrogen Sensors on the Basis of SnO2–TiO2 Systems. Sens. Actuators B: Chem. 2012, 174, 527–534.
72. Plecenik, T.; Moško, M.; Haidry, A.A.; Ďurina, P.; Truchlý, M.; Grančič, B.; Gregor, M.; Roch, T.; Satrapinskyy, L.; Mošková, A.; et al. Fast Highly-Sensitive Room-Temperature Semiconductor Gas Sensor Based on the Nanoscale Pt–TiO2–Pt Sandwich. Sens. Actuators B Chem. 2015, 207, 351–361.